ELASTICITY IMAGING OF THE LIVER: IS A HEMANGIOMA HARD OR SOFT?

S.Y. Emelianov,[1,3] J.M. Rubin,[2] M.A. Lubinski,[1] A.R. Skovoroda[3] and M. O'Donnell[1]

[1] Biomedical Engineering and [2] Radiology Departments, University of Michigan, Ann Arbor, MI 48109, USA, and
[3] Institute of Mathematical Problems in Biology, Russian Academy of Sciences, Pushchino 142292 Russia

Abstract – Diagnosing hemangioma - the most common benign vascular malformation in the liver - requires special and expensive imaging studies including nuclear medicine, magnetic resonance or CT scans. Routine ultrasound is suggestive but not diagnostic. In this paper, we test the hypothesis that hemangioma can be diagnosed using ultrasound-based reconstructive elasticity imaging. A hemangioma consists of large, blood-filled, endothelial-lined spaces separated by fibrous septa. Internally, hemangiomata are soft and spongy. Imaging the elasticity of liver using ultrasound may differentiate hemangioma from other tumor types, and therefore, provide a non-invasive means of hemangioma diagnosis.

INTRODUCTION

Hemangioma is the most prevalent benign tumor of the liver, occurring in up to 7% of the population. Hemangiomata can vary in size and be as large as several centimeters. These tumors are filled with vascular channels of various sizes and may also contain fibrous tissue. Thrombi (clotted blood) may be present in the vascular channels. Histologically, the hemangioma is characterized by large, thin walled blood vessels completely filled with blood. Grossly, hemangiomata are soft and spongy [1].

These asymptomatic lesions are often found incidentally on ultrasound or CT when imaging studies are undertaken for other reasons. Once diagnosed, no treatment is necessary, and only large, symptomatic hemangiomata are treated by surgical resection. The diagnosis of hemangioma, however, requires special imaging studies such as nuclear medicine scans using radioactive technicium tagged red blood cells, magnetic resonance or dynamic CT scans with contrast. Rarely, a hepatic angiogram is necessary to make a definite diagnosis.

Routine ultrasound can easily detect hemangiomata. The hemangioma can be clearly identified in the B-Scan image as a hyperechoic region, and the margins of the tumor are usually well-defined. An example is presented in Fig. 2. Routine ultrasound is suggestive but usually not diagnostic, however. Many other tumors, some malignant, may appear similar on the B-Scan. Therefore, there is a need to specify a detected liver mass in the least invasive and most time/cost efficient way available.

In the literature, hemangiomata are often referred to as soft and spongy lesions filled with blood [1]. Therefore, elasticity imaging may help to diagnose hemangioma. Indeed, most tumors are usually harder compared to the background, and therefore, hemangioma may be easily distinguished from other liver tumors based on its mechanical properties.

MATERIALS AND METHODS

To test the hypothesis that elasticity imaging can detect and diagnose hemangioma, studies on volunteers with previously diagnosed hemangioma were initiated. In these experiments, the liver was imaged between the ribs using an Ultramark-9 ATL scanner with a linear 128 element array transducer operating at 5 MHz. The system was interfaced to a custom-made circuit board to acquire approximately 120 frames of real-time digital RF signals during 4 seconds [2]-[3]. Within this interval, the array, attached to a deformational device residing on a clinical trolley (gurney), was pressed against the body to produce modest deformation of the liver (see Fig. 1). In most experiments, surface deformations did not exceed 10-12 mm, and all volunteers indicated no discomfort from the applied stress.

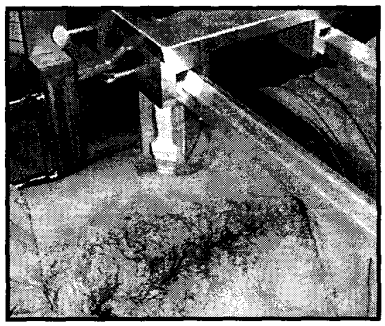

Figure 1: Clinical elasticity imaging system.

Clinical results were verified using a gel based phantom mimicking hemangioma. In this block-shaped

0-7803-4095-7/98/$10.00

phantom, the lesion was produced by a thin, acoustically transparent plastic tube (25 mm diameter and 200 μm wall thickness) filled with gelatin. Precisely the same gelatin was used inside of the tube and in the background material. Therefore, there is no elasticity difference between the lesion (i.e., internal) and surrounding (i.e., background) materials. The tube was positioned approximately in the middle of the phantom with its longitudinal axis perpendicular to the imaging plane so that the circular cross-section of the tube was imaged during deformation. Deformations were applied from the top using a similar setup to that depicted in Fig. 1. The bottom of the phantom was constrained.

In all experiments, frame-to-frame motion was estimated using a two-dimensional correlation-based phase-sensitive speckle tracking technique [2]-[3]. The 2-D displacement was estimated from the position of the maximum correlation coefficient, where the axial displacement estimate was refined using the position of the zero crossing of the analytic signal correlation [2]. Displacement error was further reduced by filtering spatially adjacent correlation functions prior to displacement estimation. Finally, frame-to-frame estimates of displacement and strain were combined to create displacement and strain images with high signal-to-noise ratios [3]-[4].

STRAIN IMAGING

The B-Scan image of a liver hemangioma is presented in Fig. 2a. This image is typical, where the location, margins and size of the tumor are clearly identified. The images in Fig. 2 are 38-mm by 78-mm, where the transducer is located at the top of the image. The muscle layers can be easily recognized at the top.

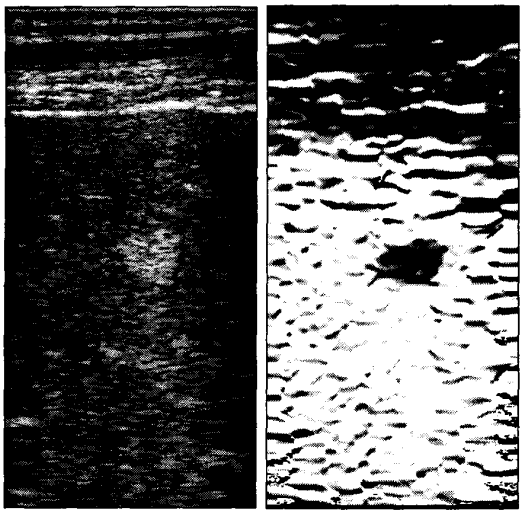

Figure 2: Hemangioma B-Scan (left) and strain image (right).

The distribution of the normal axial strain (ε_{22}) is shown in Fig. 2b. This quantitative grayscale image is displayed from 0 to 10 percent strain, where full black corresponds to no strain and full white to 10% strain. The tumor is clearly visible as a low strain region indicating that it is **harder** overall than the background tissue.

Similar results were obtained from several other volunteers. The apparent overall hardness of a hemangioma is unexpected given the soft interior of the tumor. However, this result is consistent with palpatory information gathered by surgeons in the operating room - when large, symptomatic hemangiomata are treated by surgical resection, the intact hemangiomata are felt as hard lesions. Pressure applied to the hemangioma, however, ruptures it, releasing blood as it collapses. Therefore, a hemangioma feels hard even it is filled with blood, which has no shear elasticity (i.e., soft).

In general, a soft, fluid-filled sack can appear hard if it is encapsulated by a very hard, thin membrane. If the mechanical properties of the shell are similar to that of the lesion, the shell itself would not affect the strain pattern. If the shell is harder than the lesion, however, the strain magnitude reduces inside of the lesion. In fact, for an infinitely hard and absolutely non-compliant shell, the strain inside of the lesion vanishes regardless of the internal material properties. We hypothesis that the thin membrane encapsulating a hemangioma is significantly harder than the tumor core, and dominates the overall strain pattern within the tumor.

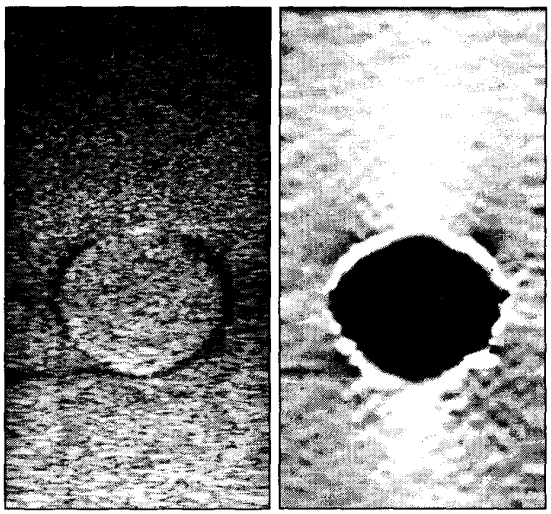

Figure 3: Phantom B-Scan (left) and strain image (right).

As an initial test of this hypothesis, we investigated strain images within the phantom mimicking a hemangioma. A B-Scan of this phantom is presented in Fig. 3a, where the thin (200 μm) plastic shell defining

the "lesion" is easily seen. Note that the material inside and outside of the lesion is the same. Figure 3b presents the normal axial strain displayed over a 0 to 15 percent dynamic range. The entire lesion appears as a low strain region, signaling that the overall lesion is harder than the background. However, the lesion contains gelatin of the **same** elastic modulus as the background material. The strain image appears very similar to that of a gel-based phantom with a single, uniform hard inclusion (published elsewhere [2]-[3], [5]).

Clearly, the mechanical properties of the shell surrounding a lesion can significantly impact the strain distribution. In particular, the strain images of a heterogeneous lesion surrounded by a hard shell and a uniform hard inclusion appear very similar. It may be possible, however, to estimate the lesion composition in both cases using reconstructive elasticity imaging.

RECONSTRUCTIVE ELASTICITY IMAGING

The problem of inverting measured displacement and strain components to reconstruct the Young's modulus can be formulated in a number of different ways [5]-[7]. For elasticity imaging of hemangioma, the reconstruction was performed using two approaches: direct reconstruction and model-based reconstruction. Direct reconstruction numerically solves the discretized equilibrium equations for a plane strain condition [6]. The plane strain condition is a reasonable approximation for elasticity imaging of the liver, where deformations are applied through the rib cage resulting in negligible out-of-plane strains. This method does not require any *a-priori* knowledge of the object, and no other assumptions are made. After defining a region of interest containing the lesion, the Young's modulus distribution is reconstructed relative to the modulus of the background tissue (i.e., liver).

If further assumptions about the geometry of the object can be made, then a more robust reconstruction can be performed [6]. Here we assume that the hemangioma can be modeled as an ellipsoid such that the elastic modulus within the imaging plane is simply a function of radial position from the center of the tumor. For a realistic tumor, this is a reasonable approximation if the tumor is not near external boundaries. Nevertheless, by assuming a simple model such as this, reconstruction in the vicinity of the tumor core is far less susceptible to strain noise than direct reconstruction.

Both reconstruction methods were first tested on the phantom, as illustrated in Fig. 4. These images represent a 30-mm by 30-mm region of interest (ROI) centered at the inclusion. The reconstructed elastic modulus is displayed on the same logarithmic scale for both approaches. Clearly, both methods identified the softer core and the hard shell.

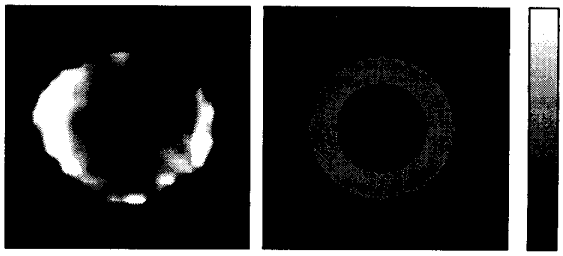

Figure 4: Elasticity images of phantom.

A quantitative comparison of direct (solid line) and model-based (dotted line) reconstruction methods is presented in Fig. 5, where the Young's modulus profiles along the center image line are shown. The agreement between these two approaches should not be too surprising for the phantom experiment since the plane strain condition was satisfied, and the geometry of the inclusion closely corresponds to the assumption made in the model-based reconstruction.

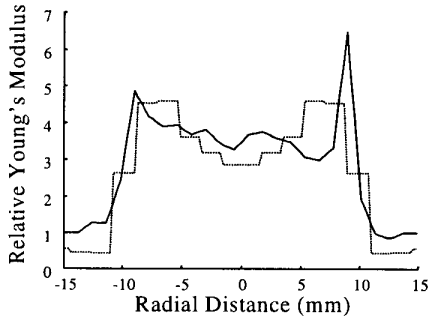

Figure 5: The Young's modulus distribution in phantom.

These reconstruction algorithms were also applied to the hemangioma. The results are presented in Fig. 6.

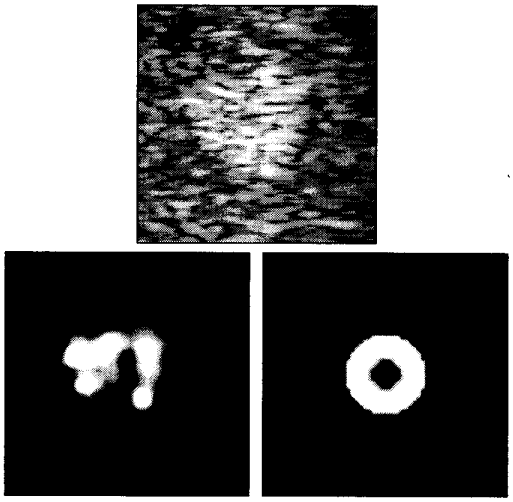

Figure 6: B-Scan and elasticity images of hemangioma.

In figure 6a, a 17.5-mm by 17.5-mm region of interest (ROI) containing the hemangioma is shown. For direct reconstruction (Fig. 6b), the Young's modulus along the ROI boundary was set to unity, resulting in reconstruction of the Young's modulus relative to liver. Clearly, the overall hemangioma is harder than the background tissue, but it has a softer interior part. This distribution is better depicted in the model-based elasticity image (Fig. 6c), where the softer interior part can be easily identified.

Finally, the Young's modulus distributions along the horizontal line intersecting the center of the hemangioma are contrasted in Fig. 7 indicating good agreement between the two different reconstruction approaches.

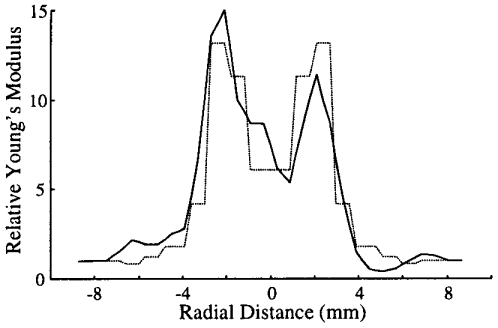

Figure 7: The Young's modulus distribution in hemangioma.

The results in Figs. 6 and 7 correspond closely to the expected elasticity distribution within the hemangioma, where the capsule surrounding the tumor makes the lesion harder overall. Reconstructive elasticity imaging captures the complex composition of such tumors.

DISCUSSION AND CONCLUSIONS

The results of this study suggest that diagnosis of liver hemangioma may be possible with reconstructive elasticity imaging. Strain imaging by itself may not be sufficient to differentiate a hemangioma from other types of liver tumors since all can produce somewhat similar strain images.

In phantom studies, the reconstructed elasticity inside and outside of the lesion was not the same even though the material was the same. There are two reasons for this. First, reconstruction algorithms are sensitive to noise in strain measurements. Second, current reconstruction algorithms eliminate the static pressure from the elasticity equilibrium equations since it is difficult to measure remotely. The harder the shell surrounding the lesion, however, the more information regarding the lesion composition is contained in the internal static pressure distribution. Ultimately, for an absolutely hard shell, only the internal pressure distribution can differentiate it from an absolutely hard uniform inclusion.

Future studies will be directed towards detailed clinical testing of reconstructive ultrasound elasticity imaging for hemangioma diagnosis.

ACKNOWLEDGEMENTS

Support from the National Institutes of Health under Grant DK 47324 is gratefully acknowledged. Many thanks to ATL for the "Ultramark-9" HDI imaging system. The authors also would like to thank John Crowe for the parallel processing software used in displacement and strain computations.

REFERENCES

[1] R.S. Cotran, V. Kumar, S.L. Robbins, *Robbins Pathologic Basis of Disease*. Philadelphia: W.B. Saunders, 1994, 5th edition.

[2] M. Lubinski, S. Emelianov, and M. O'Donnell, "Speckle tracking methods for ultrasonic elasticity imaging using short time correlation," accepted for publication in *IEEE Transactions on Ultrasonics, Ferroelectrics, and Frequency Control,* 1998.

[3] M.A. Lubinski, S. Emelianov, and M. O'Donnell, "Adaptive strain estimation using retrospective processing," accepted for publication in *IEEE Transactions on Ultrasonics, Ferroelectrics, and Frequency Control,* 1998.

[4] M. O'Donnell, S.Y. Emelianov, A.R. Skovoroda, M.A. Lubinski, W.F. Weitzel, and R.C. Wiggins, "Quantitative elasticity imaging," in *Proceedings of the 1993 IEEE Ultrasonics Symposium*, 1993, vol. 2, pp. 893-903.

[5] A.R. Skovoroda, M.A. Lubinski, S.Y. Emelianov, and M. O'Donnell, "Reconstructive elasticity imaging for large deformations," submitted for publication in *IEEE Transactions on Ultrasonics, Ferroelectrics, and Frequency Control*, 1998.

[6] A.R. Skovoroda, S. Emelianov, and M. O'Donnell, "Reconstruction of tissue elasticity based on ultrasound displacement and strain images," *IEEE Transactions on Ultrasonics, Ferroelectrics, and Frequency Control*, 42, pp. 747-765, 1995.

[7] A.R. Skovoroda, S.Y. Emelianov, M.A. Lubinski, A.P. Sarvazyan and M. O'Donnell, "Theoretical analysis and verification of ultrasound displacement and strain imaging," *IEEE Transactions on Ultrasonics, Ferroelectrics, and Frequency Control*, 41, pp. 302-313, 1994.